

Time Resolved Fluorescence and Energy Transfer Analysis of Nd^{3+} – Yb^{3+} – Er^{3+} Triply-Doped Ba–Al–Metaphosphate Glasses for an Eye Safe Emission (1.54 μm)

Atul D. Sontakke · Kaushik Biswas · Ashis K. Mandal · Kalyandurg Annapurna

Received: 31 July 2009 / Accepted: 12 October 2009 / Published online: 23 October 2009
© Springer Science + Business Media, LLC 2009

Abstract This paper reports on the preparation and systematic analysis of energy transfer mechanisms in Nd^{3+} – Yb^{3+} – Er^{3+} co-doped new series of barium-alumino-metaphosphate glasses. The time resolved fluorescence of Nd^{3+} in triply doped Ba–Al–metaphosphate glasses have revealed that, Yb^{3+} ions could function as quite efficient bridge for an energy transfer between Nd^{3+} and Er^{3+} ions. As a result, a fourfold emission enhancement at 1.54 μm of Er^{3+} ions has been achieved through an excitation of $^4\text{F}_{5/2}$ level of Nd^{3+} at 806 nm for the glass having 3 mol% Yb^{3+} with an energy transfer efficiency reaching up to 94%. Decay of donor (Nd^{3+}) ion fluorescence has been analyzed based on theoretical models such as direct energy transfer model (Inokuti–Hirayama) and migration assisted energy transfer models (Burshtein’s hopping and Yokota–Tanimoto’s diffusion). The corresponding energy transfer parameters have been evaluated and discussed. Primarily, electrostatic dipole–dipole ($s\sim 6$) interactions are found to be responsible for the occurrence of energy transfer process in these glasses.

Keywords Metaphosphate glasses · Energy transfer · Fluorescence · Sensitized Er^{3+} NIR emission

Introduction

Sensitized emission occurrence from the lanthanide ions (Ln^{3+}) has attracted significant attention and importance.

The energy transfer efficiency among donor-acceptor ions depends on overlapping of donor’s emission with that of activator’s absorption and their inter-ionic distances. Hence, heavily doped solid-state gain media including laser crystals, glasses and rare earth doped fibers have recently been considered more relevant for energy transfer luminescence studies. A great deal of work has been carried out in exploring the energy transfer amongst lanthanides ($\text{RE}^{3+} \rightarrow \text{RE}^{3+}$) as well as transition metal ions with lanthanides ($\text{TM} \rightarrow \text{RE}^{3+}$) ions in the visible (VIS) region [1–3]. The main interest of those works has been focused on rare earth ions like Eu^{3+} , Tb^{3+} , which could be sensitized by UV absorbing Ce^{3+} , Gd^{3+} ions for their potential use in lighting, display and dosimetric applications [4, 5]. With the emergence of laser diodes, the interest has been extended towards the NIR emitting ions like Pr^{3+} , Nd^{3+} , Tm^{3+} , Ho^{3+} , Er^{3+} and Yb^{3+} etc. NIR emission plays an important role in optical communications, biomedical applications and lasers [6, 7] such as Nd^{3+} based laser systems, which are well known for their high power applications [8]. However, for certain singly doped ions, like Yb^{3+} based lasers, various technical problems arise for high power operation; since the energy difference between excitation and emission is very small due to its two level configurations [9]. Some attempts have been made earlier in finding a suitable glass host so as to bring in a wider separation from the Stark components of lower energy states of Yb^{3+} resulting in with a quasi-three level system [10]. Yet another good solution to overcome this difficulty is to sensitize it with Nd^{3+} ion so as to achieve an efficient lasing at 980 nm from Yb^{3+} on exciting the Nd^{3+} ion with easily available high power 800 nm laser diode [11, 12]. Beside its lasing performance, Yb^{3+} serves as good sensitizer for several lanthanides (Pr^{3+} , Ho^{3+} , Tm^{3+} , Er^{3+} etc.) because of its high absorption and emission cross-

A. D. Sontakke · K. Biswas · A. K. Mandal · K. Annapurna (✉)
Glass Technology Laboratory, Council of Scientific and Industrial
Research, Central Glass and Ceramic Research Institute,
196, Raja S.C. Mullick Road,
Kolkata 700032, India
e-mail: glasslab42@hotmail.com

section in combination with higher allowed doping concentrations. Its sensitization is based on either resonant energy transfer (RET) or phonon-assisted energy transfer (PAET) for improved NIR emission and energy transfer upconversion (ETU) for visible emissions from activator ions [13, 14]. Among these, Er^{3+} possesses special interest due to its NIR emission at eye safe wavelength (1.53 μm). In addition, it has been recognized as one of the most efficient rare earth ions to be used in optical communication and range finder applications since its emission coincides with the third communication/atmospheric window (1.525–1.565 μm) [15]. For Nd^{3+} – Yb^{3+} or Yb^{3+} – Er^{3+} systems, the energy transfer is more or less resonant since the emission of sensitizer overlaps with absorption of activator and such systems have been widely studied. However, very few reports are available on Nd^{3+} sensitization to Er^{3+} ions [16]. Moreover, in this system it was found that the spectral energy mismatch of 1,150 cm^{-1} does exist between donor (Nd^{3+}) and acceptor (Er^{3+}) and hence phonon assisted energy transfer may be responsible for this process. Since Yb^{3+} ions can act as activators for Nd^{3+} and very efficient sensitizers for Er^{3+} , it can be expected to achieve improved energy transfer from Nd^{3+} to Er^{3+} in the presence of Yb^{3+} as bridging ions. An attempt has been made to examine the $\text{Nd}^{3+} \rightarrow \text{Er}^{3+}$ energy transfer with the presence and absence of Yb^{3+} ions in alkali free Barium-alumino-metaphosphate glass host.

Metaphosphate glasses are advantageous over silicate and other host glasses for their high rare earth ion doping concentration without considerable fluorescence quenching along with possessing low melting temperature and several favorable spectroscopic properties including high emission cross-sections and longer fluorescence lifetime of active ions and hence have been used in the development of high power solid-state lasers [17]. Among them, sodium phosphate, barium phosphate, alumino-metaphosphate and potassium-alumino-metaphosphate glasses have been studied widely [18–21]. In addition to these several other metaphosphate glasses including Zn- or Pb-metaphosphate have also been investigated for their optical and spectroscopic properties in the presence of active ions [22]. However, to our knowledge, there are no reports so far on alkali free barium-alumino-metaphosphate glass system in the literature.

Hence, in the present work our main objective is to prepare a new series of alkali free barium-alumino-metaphosphate glasses containing mono, bi and tri rare earth ions (Nd^{3+} – Yb^{3+} – Er^{3+}) and to examine the intermediate Yb^{3+} ion influence on the sensitization efficiency of Nd^{3+} for NIR emission from Er^{3+} ions. The energy transfer mechanism between Nd^{3+} and Er^{3+} ions in the presence and absence of Yb^{3+} has been systematically analyzed from the measurement of photoluminescence spectra and the time

resolved decay profiles of these new series of optical glass systems by employing theoretical models.

Experimental study

The glasses in the following chemical compositions (in mole %) were developed by employing melt quenching method:

1. **BAP-Nd**: 11.60 Al_2O_3 –20.73 BaO –55.54 P_2O_5 –6.72 SiO_2 –3.86 B_2O_3 –0.5 Nb_2O_3 –1.05 Nd_2O_3
2. **BAP-Er**: 11.60 Al_2O_3 –20.73 BaO –55.54 P_2O_5 –6.72 SiO_2 –3.86 B_2O_3 –0.5 Nb_2O_3 –1.05 Er_2O_3
3. **BAP-NdEr**: 11.47 Al_2O_3 –20.51 BaO –54.95 P_2O_5 –6.64 SiO_2 –3.83 B_2O_3 –0.5 Nb_2O_3 –1.05 Nd_2O_3 – 1.05 Er_2O_3
4. **BAP-NdYb**: 11.48 Al_2O_3 –20.52 BaO –54.97 P_2O_5 –6.65 SiO_2 –3.83 B_2O_3 –0.5 Nb_2O_3 –1.05 Nd_2O_3 –1.0 Yb_2O_3
5. **BAP-Yb05**: 11.42 Al_2O_3 –20.41 BaO –54.66 P_2O_5 –6.61 SiO_2 –3.80 B_2O_3 –0.5 Nb_2O_3 –1.05 Nd_2O_3 –1.05 Er_2O_3 –0.5 Yb_2O_3
6. **BAP-Yb10**: 11.36 Al_2O_3 –20.30 BaO –54.39 P_2O_5 –6.58 SiO_2 –3.78 B_2O_3 –0.49 Nb_2O_3 –1.05 Nd_2O_3 –1.05 Er_2O_3 –1.0 Yb_2O_3
7. **BAP-Yb20**: 11.24 Al_2O_3 –20.10 BaO –53.81 P_2O_5 –6.51 SiO_2 –3.75 B_2O_3 –0.49 Nb_2O_3 –1.05 Nd_2O_3 –1.05 Er_2O_3 –2.0 Yb_2O_3
8. **BAP-Yb30**: 11.12 Al_2O_3 –19.88 BaO –53.27 P_2O_5 –6.44 SiO_2 –3.71 B_2O_3 –0.48 Nb_2O_3 –1.05 Nd_2O_3 –1.05 Er_2O_3 –3.0 Yb_2O_3

Reagent grade metaphosphate chemicals such as $\text{Ba}(\text{PO}_3)_2$ and $\text{Al}(\text{PO}_3)_3$ and high purity rare earth oxides, Nd_2O_3 , Er_2O_3 and Yb_2O_3 with purity 99.99% from Alpha-Aesar were used as raw materials for glass preparation. Special precautions were taken in controlling the hydroxyl ion (OH^-) contents in prepared glasses by sintering the batches and maintaining the relative atmospheric humidity (RH) below 40%. Thus thoroughly mixed chemical batches were sintered at 350 $^\circ\text{C}$ for 6 h to reduce the surface absorbed moisture and to make pre-reacted batch. Each sintered batch was then melted at 1,350 $^\circ\text{C}$ in silica crucibles for 1 h with intermittent stirrings to get homogeneity and later casted them onto preheated graphite molds. The glass samples thus obtained were kept for annealing at 550 $^\circ\text{C}$ to relieve thermal stresses and cooled slowly to room temperature in a precise temperature controlled annealing furnace. Such annealed glasses were cut and polished in the form of plates in the dimensions of 15 \times 20 \times 2 mm^3 for optical characterizations.

The densities of all glasses were measured by employing the Archimedes buoyancy principle using water as buoyancy liquid. Refractive indices of glasses were measured at

five different wavelengths (473 nm, 532 nm, 632.8 nm, 1,060 nm and 1,552 nm) on Metricon M2010 Prism Coupler equipped with laser sources.

The UV-Vis optical absorption spectra of the Nd^{3+} , Yb^{3+} , Er^{3+} singly and co-doped barium-alumino-metaphosphate glasses were recorded on a UV-Vis spectrophotometer (Model: Lambda20, Perkin-Elmer) in the range of 200–1,100 nm. The Fluorescence emission, excitation, and decay measurements were carried out on Fluorescence spectrophotometer (Model: Quantum Master, enhanced NIR, from Photon Technologies International) fitted with double monochromators on both excitation and emission channels. The instrument is equipped with LN_2 cooled gated NIR photo-multiplier tube (Model: NIR-PMT-R1.7, Hamamatsu) as detector for acquiring both study state spectra and phosphorescence decay. For decay measurements, a 60 W Xenon flash lamp was employed as an excitation source.

Results and discussion

Physical and optical properties

Some of the important physical and optical properties of Nd^{3+} , Yb^{3+} , Er^{3+} doped barium-alumino-metaphosphate glasses are presented in Table 1. The density (d) and average molecular weight (M_{avg}) of glasses are found to be increasing with an increase in the dopant ion content due to inclusion of relatively heavy metal ions (RE^{3+}) in glass network. Using these values, Rare earth ion concentration (N_{RE}), Inter-ionic distance (r_i), Polaron radius (r_p) and Field strength (F) have been estimated using relevant equations [23, 24] and are listed out in the same table. The measured refractive indices of all Nd^{3+} , Yb^{3+} , Er^{3+} doped barium-alumino-metaphosphate glasses at 473 nm, 532 nm, 632.8 nm, 1,060 nm and 1,552 nm were fitted with the Sellmeire equation [25] to obtain the refractive indices at standard wavelengths, n_c (at 546.1 nm), n_F (at 480 nm) and n_C (at 643.8 nm) which have been used to calculate different optical parameters [26]. The Abbe number of all glasses is around 65–70 indicating the low optical dispersion in these glasses.

Spectral properties

Optical absorption spectra

The room temperature absorption spectra of BAP-Nd, BAP-Er and BAP-Yb10 barium-alumino-metaphosphate glasses are shown in Fig. 1 as representative curves. The spectra reveal in-homogeneously broadened absorption bands due to $f-f$ electronic transitions from Nd^{3+} , Yb^{3+}

and Er^{3+} ions respectively. All absorption peaks have been appropriately assigned depending upon their peak energies [27]. For BAP-Nd glass doped with Nd^{3+} ions, the absorption peaks centered at 327 nm, (348 nm, 356 nm), 429 nm, 472 nm, (510 nm, 523 nm), 582 nm, 627 nm, 683 nm, 746 nm, 803 nm and 874 nm wavelengths have been detected and were assigned to transitions from ground state $^4I_{9/2}$ to the higher excited states $^4D_{7/2}$, ($^4D_{5/2}$, $^4D_{1/2}$), $^2P_{1/2}$, $^2G_{9/2}$, ($^4G_{9/2}$, $^4G_{7/2}$), ($^4G_{5/2}$, $^2G_{7/2}$), $^2H_{11/2}$, $^4F_{9/2}$, ($^4F_{7/2}$, $^4S_{3/2}$), ($^4F_{5/2}$, $^2H_{9/2}$) and $^4F_{3/2}$ respectively of Nd^{3+} $4f^8$ electronic configuration. In the case of BAP-Er glass, the absorption peaks at 364 nm, 377 nm, 405 nm, 450 nm, 487 nm, 520 nm, 545 nm, 650 nm, 802 nm and 974 nm are designated to the transitions $^4I_{15/2} \rightarrow ^4G_{7/2}$, $^4G_{11/2}$, $^2G_{9/2}$, $^4F_{5/2}$, $^4F_{7/2}$, $^2H_{11/2}$, $^4S_{3/2}$, $^4F_{9/2}$, $^4I_{9/2}$ and $^4I_{11/2}$ of $4f^7$ configuration of Er^{3+} ions respectively. The absorption spectrum for BAP-Yb10 glass sample, which is triply doped with Nd^{3+} , Er^{3+} and Yb^{3+} , has exhibited respective transitions from each dopant ion. Besides the Nd^{3+} and Er^{3+} absorption peaks, an intense absorption band at 974 nm with shoulders at 914 nm and 950 nm is due to a transition from ground state $^2F_{7/2}$ to $^2F_{5/2}$ and its corresponding stark energy levels respectively of Yb^{3+} ions [28]. From the absorption spectrum of BAP-Yb10, it has been noticed that there exists a slight increase in bandwidths of certain absorption peaks (as indexed with mixed transitions in Fig. 1) due to the absorption overlapping of different ions. From all these absorption spectra, it can be seen that absorption band due to $^4I_{9/2} \rightarrow ^4F_{5/2}$ of Nd^{3+} at 803 nm has prominently been intense which could be availed to excite the Nd^{3+} singly and co-doped glasses for rich emissions from them.

Photoluminescence emission and excitation spectra

The room temperature photoluminescence spectra of Nd^{3+} singly, Nd^{3+} - Er^{3+} co-doped and Nd^{3+} - Yb^{3+} - Er^{3+} triply-doped barium-alumino-metaphosphate glasses obtained upon 806 nm excitation at $^4F_{5/2}$ level of Nd^{3+} ions and $^4I_{9/2}$ level of Er^{3+} are presented in Fig. 2. The emission bands centered at 887 nm, 1,058 nm and 1,324 nm are attributed due to transitions $^4F_{3/2} \rightarrow ^4I_{9/2, 11/2}$ and $13/2$ respectively of Nd^{3+} and the bands at 976 nm, 1,542 nm are ascribed to transitions $^2F_{5/2} \rightarrow ^2F_{7/2}$ of Yb^{3+} and $^4I_{13/2} \rightarrow ^4I_{15/2}$ of Er^{3+} respectively [12, 29]. All the spectra have been normalized with respect to Nd^{3+} emission at 1,058 nm. The inset figure depicts a histogram representing the variation of fluorescence intensity of transition $^4F_{3/2} \rightarrow ^4I_{11/2}$ (Nd^{3+}) and $^4I_{13/2} \rightarrow ^4I_{15/2}$ (Er^{3+}) for different samples. It can be clearly seen that the emission intensity of Nd^{3+} decreased, while that of Er^{3+} increased on Nd^{3+} - Er^{3+} co-doping and this trend continues in the samples with the inclusion followed by successive concentration increase of

Table 1 Important physical and optical properties; density (d), average molecular weight (M_{avg}), molar volume (V_M), concentration of dopant ions (N_{RE} in 10^{20} ions/cm³), inter-ionic distance (r_i), polaronradius (r_p), field strength (F), refractive index (n_e , n_F and n_C), Abbe number (ν_e) and reflection loss ($R\%$) of different Nd³⁺, Yb³⁺, Er³⁺ doped barium-alumino-metaphosphate glasses

Glass	BAP-Nd	BAP-Er	BAP-NdEr	BAP-Yb05	BAP-Yb10	BAP-Yb20	BAP-Yb30
Physical properties							
d (g/cm ³)	3.037	3.033	3.060	3.095	3.101	3.150	3.184
M_{avg} (g/mol)	134.1	134.5	136.7	138.0	139.3	142.0	144.6
V_M (cm ³)	44.1	44.4	44.6	44.6	44.9	45.1	45.4
N_{Nd}	2.88	–	2.844	2.835	2.824	2.820	2.799
N_{Er}	–	2.865	2.844	2.835	2.824	2.820	2.799
N_{Yb}	–	–	–	1.353	2.677	5.345	7.960
r_i (Å)	15.14	15.17	12.07	11.25	10.63	9.69	9.03
r_p (Å)	6.10	6.11	4.86	4.53	4.28	3.91	3.64
F (10^{14} cm ⁻²)	8.06	8.03	12.68	14.59	16.34	19.66	22.63
Optical properties							
n_e	1.5529	1.5512	1.5532	1.5534	1.5546	1.5554	1.5559
n_F	1.5567	1.5549	1.5571	1.5574	1.5587	1.5595	1.5601
n_C	1.5488	1.5471	1.5491	1.5493	1.5504	1.5512	1.5516
ν_e	70.0	70.6	69.3	68.7	67.2	66.9	65.4
$R\%$	4.69	4.67	4.69	4.70	4.71	4.72	4.73

Yb³⁺ ions. An enhancement of Er³⁺ emission intensity has reached a four-fold for BAP-Yb30 sample. The increased Er³⁺ emission from co-doped samples clearly signifies the occurrence of energy transfer from Nd³⁺ to Er³⁺ in these glasses, which increases with the increase in Yb³⁺ concentration. The mechanism involved in this energy transfer process can be understood on close examination of recorded excitation spectra for Er³⁺, Yb³⁺ and Nd³⁺ emissions as shown in Fig. 3a–c respectively. Figure 3a presents the excitation spectra of glasses in the wavelength

range of 350–1,000 nm by monitoring Er³⁺ emission at 1,542 nm. The spectra revealed different excitation bands from all dopant Er³⁺, Nd³⁺ and Yb³⁺ ions. The presence of both Nd³⁺ and Yb³⁺ excitation peaks in these spectra indicates their sensitization ability for Er³⁺ emission. On critical examination of these trends, it has been observed that, the excitation intensity due to both Nd³⁺ and Yb³⁺ increases with an increase in Yb³⁺ content; however, the Er³⁺ excitation intensity remains unchanged. This observed increase in the Nd³⁺ excitation intensity with an increase in Yb³⁺ concentration clearly indicates the active role played by Yb³⁺ in Nd³⁺ → Er³⁺ energy transfer.

For Nd³⁺–Er³⁺ co-doped system, the energy transfer suggested by Shi et al. [16] and by other authors [30] follows the mechanism (Nd³⁺: ⁴F_{3/2} + Er³⁺: ⁴I_{15/2}) → (Nd³⁺: ⁴I_{15/2} + Er³⁺: ⁴I_{13/2}). In the present glass host, energy difference between these transitions is found to be around 1,150 cm⁻¹. This clearly implies that the energy transfer from Nd³⁺ to Er³⁺ is not resonant but involves one or more phonons. With the inclusion of Yb³⁺, the energy transfer can occur from Nd³⁺ to Er³⁺ following the path Nd³⁺ → Yb³⁺ → Er³⁺ as Yb³⁺ is a well-known sensitizer for Er³⁺. The Nd³⁺ sensitization for Yb³⁺ can be evidenced from the recorded excitation spectrum by monitoring Yb³⁺ emission at 997 nm as depicted in Fig. 3b, which exhibited the excitation bands due to both Yb³⁺ and Nd³⁺ ions. Though the ⁴I_{11/2} level of Er³⁺ and ²F_{5/2} level of Yb³⁺ are in resonance with each other, the possibility of energy back transfer from Er³⁺ to Yb³⁺ is less owing to the quick relaxation of ⁴I_{11/2} level of Er³⁺ to the lower level ⁴I_{13/2}

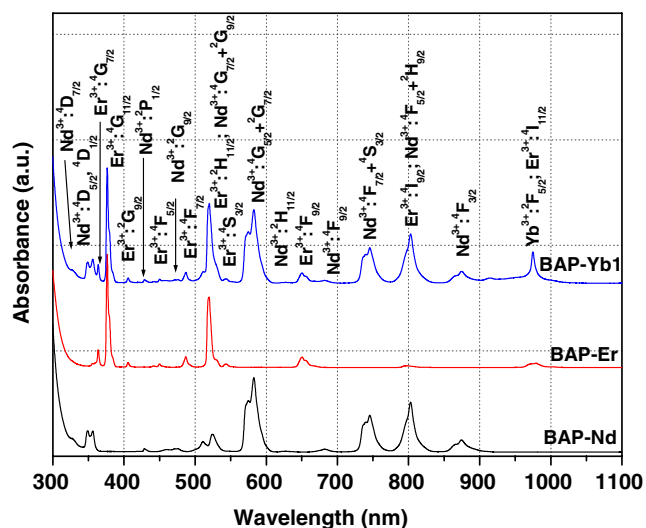


Fig. 1 Room temperature optical absorption spectra of BAP-Nd, BAP-Er and BAP-Yb10 singly and triply-doped barium-alumino-metaphosphate glasses

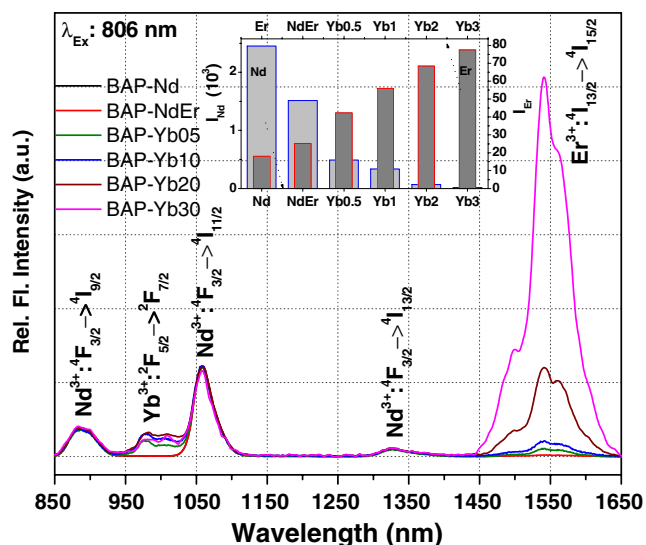


Fig. 2 Normalized luminescence spectra for singly and Nd³⁺–Yb³⁺–Er³⁺ co-doped barium-alumino-metaphosphate glasses with 806 nm excitation. (Inset: Histogram for Nd³⁺ and Er³⁺ emission for varying co-dopant concentrations.)

[31]. This can be realized from the absence of Er³⁺ excitation bands for Yb³⁺ emission in Fig. 3b. The excitation spectra obtained by monitoring the Nd³⁺ emission at 1,058 nm is presented in Fig. 3c. The spectra show the excitation bands due to transitions from ground state ⁴I_{9/2} to different excited levels of Nd³⁺ ions only. From this spectrum it is noticed that, the intensity of excitation peaks decreases with the inclusion of Er³⁺ and Yb³⁺ ions in glass matrix. This decrease in excitation intensity on co-doping with Er³⁺ and Yb³⁺ is attributed to the energy transfer from excited Nd³⁺ ions to the nearest Yb³⁺ and Er³⁺ ions. Also, there are no excitation peaks due to Yb³⁺ or Er³⁺ for Nd³⁺ emission. Thus pointing out that, even as there is an efficient energy transfer from Nd³⁺ to Yb³⁺ and in turn to Er³⁺, no evidence of back energy transfer to Nd³⁺ from Yb³⁺ and Er³⁺ has been observed.

The emission spectra of Nd³⁺ singly-doped (BAP-Nd), Nd³⁺–Yb³⁺ co-doped (BAP-NdYb) and Nd³⁺–Yb³⁺–Er³⁺ triply-doped (BAP-Yb10) barium-alumino-metaphosphate glasses in Fig. 4, gives more clear understanding on the energy transfer among these ions. For Nd³⁺ singly doped glass, the emission spectrum exhibits three distinct Nd³⁺ emission peaks at 887 nm, 1,058 nm and 1,324 nm of the transitions ⁴F_{3/2} → ⁴I_{9/2}, ^{11/2} & ^{13/2} respectively as discussed earlier. For Nd³⁺–Yb³⁺ co-doped glass, a strong and broad emission band due to Yb³⁺ appears at around 1 μm in addition to the three Nd³⁺ emission peaks. The emission peak at 1,058 nm shows an increase in intensity for BAP-NdYb glass, may be due to overlapping of Yb³⁺ emission stark components with it. This strong emission from Yb³⁺ upon Nd³⁺ excitation at 806 nm is due to Nd³⁺ → Yb³⁺

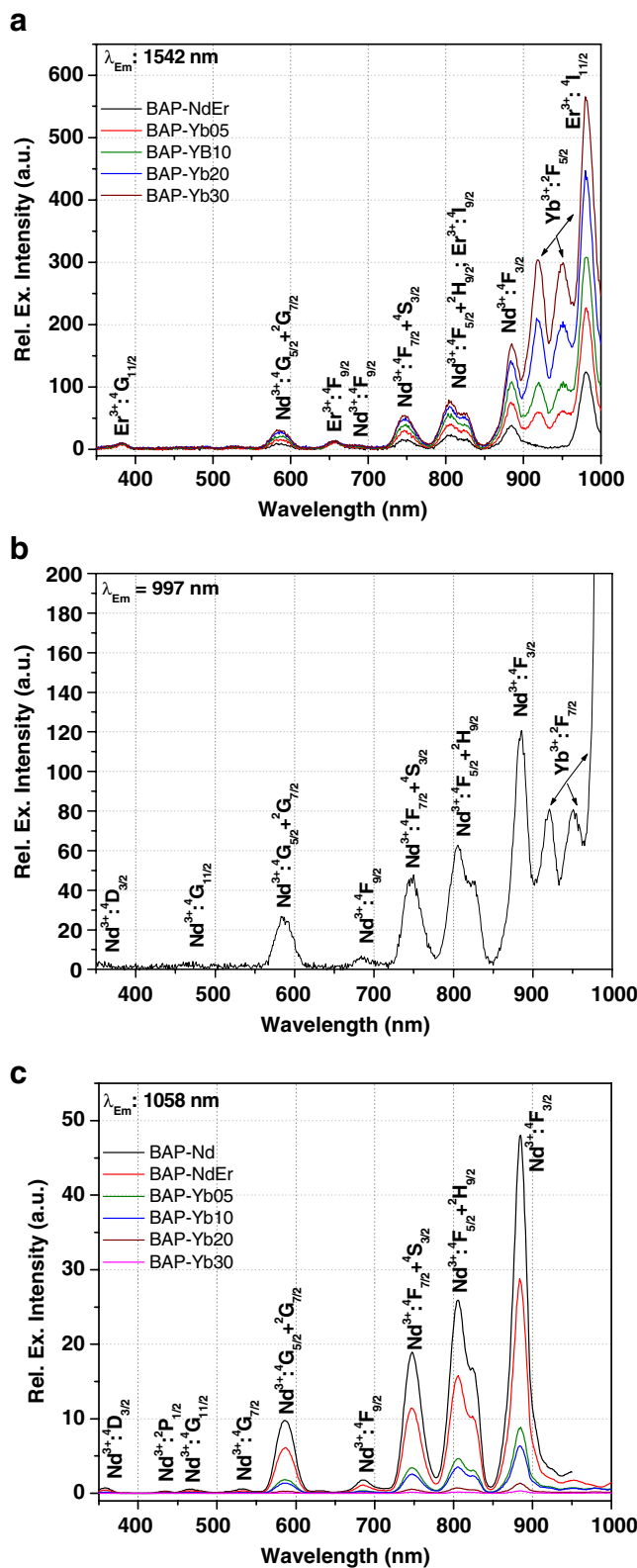


Fig. 3 Excitation spectra of Nd³⁺–Yb³⁺–Er³⁺ triply-doped barium-alumino-metaphosphate glasses upon monitoring the Er³⁺ emission at 1,542 nm (a), Yb³⁺ emission at 997 nm (b) and Nd³⁺ emission at 1,058 nm (c)

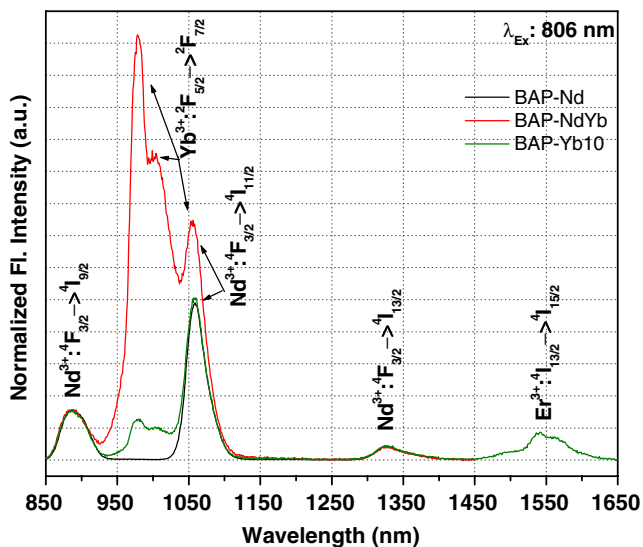


Fig. 4 Normalized emission spectra of BAP-Nd, BAP-NdYb and BAP-Yb10 glasses

energy transfer in these glasses. However, on further doping with Er³⁺ (BAP-Yb10 sample), the Yb³⁺ emission intensity decreases drastically and that of Er³⁺ emission appeared at 1.54 μm. Thus, the energy transfer in the present Nd³⁺–Yb³⁺–Er³⁺ triply-doped barium-alumino-metaphosphate glasses follows the path Nd³⁺ → Yb³⁺ → Er³⁺ as shown in the partial energy level diagram, Fig. 5. On excitation with 806 nm at ⁴F_{3/2} level of Nd³⁺, it relaxes non-radiatively to the ⁴F_{3/2} level which then transfers the energy to Er³⁺ via Yb³⁺ in addition to the mechanism suggested by Shi et al. [16] for Nd³⁺ → Er³⁺ direct energy transfer.

Fluorescence decay spectra

As the energy transfer takes place from ⁴F_{3/2} level of Nd³⁺, the decay analysis can be carried out with ⁴F_{3/2} → ⁴I_{9/2} and

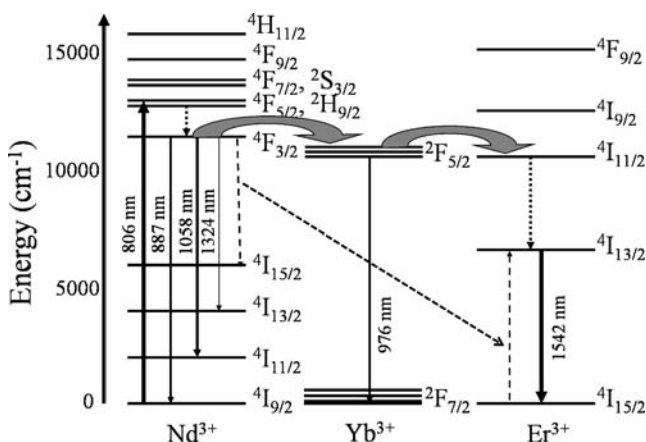


Fig. 5 Partial energy level diagram for the energy transfer mechanism from Nd³⁺, Yb³⁺ and Er³⁺ doped in barium-alumino-metaphosphate glasses

⁴F_{3/2} → ⁴I_{11/2} transitions at 887 and 1,058 nm respectively. Since ⁴F_{3/2} → ⁴I_{11/2} transition overlaps with Yb³⁺ emission, the ⁴F_{3/2} → ⁴I_{9/2} transition at 887 nm has been selected for decay analysis in this system. Figure 6 shows the time resolved fluorescence decay function of Nd³⁺ emission at 887 nm. From this figure it can be seen that, the Nd³⁺ fluorescence decays rapidly on co-doping with Er³⁺ and Yb³⁺. For Nd³⁺ singly doped sample, the decay curve is nearly single exponential with lifetime of 282 μsec. However, the exponential nature decreased with the co-doping of Er³⁺ and Yb³⁺ in these glasses. The average fluorescence lifetime (τ_{avg}) of ⁴F_{3/2} excited level from non-exponential decay curves of co-doped samples has been calculated using following equation [32] and the values are tabulated in Table 2.

$$\tau_{avg} = \frac{\left(\frac{A1}{A2}\right)\tau_1^2 + \tau_2^2}{\left(\frac{A1}{A2}\right)\tau_1 + \tau_2} \tag{1}$$

where, A1 and A2 are the weight factors of τ₁ and τ₂ respectively. From decay time values, the energy transfer rate (W_{ET}) and energy transfer efficiency (η_{ET}) have been evaluated from the following expressions [33].

$$W_{ET} = \frac{1}{\tau_{avg}} - \frac{1}{\tau_D} \tag{2}$$

$$\eta_{ET} = 1 - \frac{\tau_{avg}}{\tau_D} \tag{3}$$

where, τ_D is donor luminescence decay time in the absence of acceptor ions. The energy transfer rate is found to be increasing on co-doping with Er³⁺ and Yb³⁺ and the energy transfer efficiency of as high as 94% has been obtained for

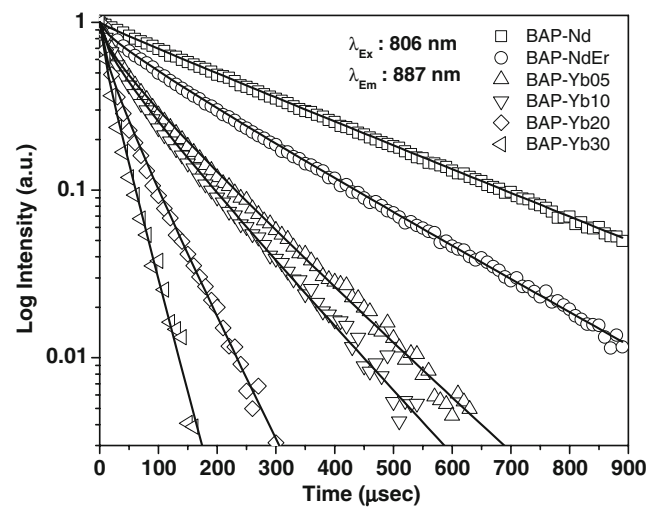


Fig. 6 Decay curves of Nd³⁺ emission at 887 nm excited at 806 nm. Solid lines are the theoretical fits using Burshtein donor energy migration model

Table 2 Measured fluorescence lifetime (τ_{avg}), energy transfer rate (W_{ET}) and energy transfer efficiency (η_{ET}) derived from decay of Nd^{3+} emission at 1,058 nm and 887 nm on 806 nm excitation

Glass	${}^4\text{F}_{3/2} \rightarrow {}^4\text{I}_{11/2}$ (1,058nm)			${}^4\text{F}_{3/2} \rightarrow {}^4\text{I}_{9/2}$ (887nm)		
	τ_{avg} (μsec)	W_{ET} (sec^{-1})	η_{ET} (%)	τ_{avg} (μsec)	W_{ET} (sec^{-1})	η_{ET} (%)
BAP-Nd	287.4	–	–	282.0	–	–
BAP-NdEr	198.1	1,567	31.1	154.2	2,939	45.3
BAP-Yb05	92.8	7,292	67.7	36.5	23,851	87.0
BAP-Yb10	79.9	9,042	72.2	27.9	32,296	90.1
BAP-Yb20	36.5	23,917	87.3	21.3	43,402	92.4
BAP-Yb30	22.9	40,209	92.1	16.4	57,429	94.2

BAP-Yb30 sample, the glass containing 3 mol% of Yb_2O_3 . Table 2 also lists the average decay times and related energy transfer parameters (W_{ET} and η_{ET}) for the emission transition ${}^4\text{F}_{3/2} \rightarrow {}^4\text{I}_{11/2}$ (at 1,058 nm) of Nd^{3+} ions. From this table it can be seen that the 887 nm emission shows more significant quenching than the emission at 1,058 nm.

In the case of donor-acceptor energy transfer, donor luminescence decay provides crucial information on the energy transfer micro-parameters and inter-ionic interactions responsible for energy transfer. Previous reports reveal that for Nd^{3+} to Er^{3+} energy transfer, the inter-ionic interaction cannot be a single but a mixture of interactions, which include exchange, dipole-dipole (d-d), dipole-quadrupole (d-q) and quadrupole-quadrupole (q-q) works together [34]. Accordingly, the decay of Nd^{3+} donor luminescence for high Er^{3+} concentration shows a fast sub-microsecond decay followed by a slow non-exponential decay and an exact fit to this decay can be obtain by considering both exchange and electrostatic (d-d, d-q and q-q) interactions contributing to the energy transfer. However, for the system with low donor-acceptor concentration, the influence of short-range interactions like exchange, d-q and q-q decreases and an acceptable fit can be obtained by considering d-d interactions only. This suggests that the energy transfer interactions strongly depend on the concentration of donor and acceptor ions, particularly on the inter-ionic distances. Shi et al. [16] demonstrated that the Nd^{3+} to Er^{3+} energy transfer is driven by d-d interactions and used Forster-Dexter model but could not give a satisfactory fit to donor luminescence decay; however, Rotman et al. [30] extended the Forster-Dexter model by assuming a non-random distribution of dopants in crystal lattice and gave a good fit by considering the excluded correlation between dopants. In the present investigation, in order to understand energy transfer mechanism involved in the Nd^{3+} - Yb^{3+} - Er^{3+} codoped system, the donor (Nd^{3+}) decay analysis has been systematically carried out on employing the direct energy transfer based Inokuti-Hirayama model and donor-donor migration assisted energy transfer models such as hopping model of Burshtein and diffusion model of Yokota-Tanimoto.

Basically the energy transfer interactions between donor (Nd^{3+}) and acceptors (Yb^{3+} , Er^{3+}) in the present glass host are found to be dipole-dipole, which has been estimated from the plot of $\ln[-\ln(I(t)/I_0)-(t/\tau_0)]$ versus $\ln(t/\tau_0)^3$ as shown in Fig. 7. The slope of the plot gives the value of ‘s’ around 6, where s is the interaction parameter whose values of 6, 8 and 10 characterize for dipole-dipole, dipole-quadrupole and quadrupole-quadrupole interactions respectively [35]. By considering the dipole-dipole interactions, decay curves have been fitted with the Inokuti-Hirayama equation [36].

$$I(t) = I_0 \exp \left[-\left(\frac{t}{\tau_0}\right) - \Gamma\left(1 - \frac{3}{s}\right) \left(\frac{C_A}{C_0}\right) \left(\frac{t}{\tau_0}\right)^{3/s} \right] \quad (4)$$

where, τ_0 is the intrinsic fluorescence decay time of the donor, $\Gamma(1-3/s)$ is Euler’s gamma function, C_A is acceptor ion concentration, C_0 is critical concentration defined as $(3/4\pi R_0^3)$ and s is the multipole interaction parameter (~6 in the present case). Figure 8 shows the fitting curves for the experimental fluorescence decay at 887 nm of BAP-NdEr,

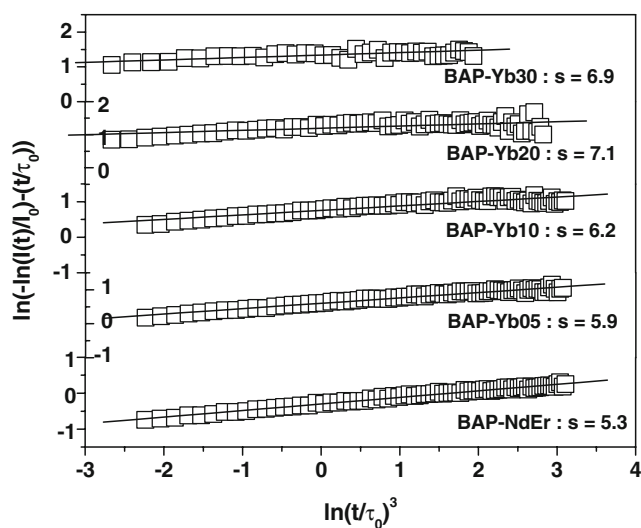


Fig. 7 Plots of experimental decay data $\ln[-\ln(I(t)/I_0)-(t/\tau_0)]$ vs. $\ln(t/\tau_0)^3$ of Nd^{3+} emission at 887 nm with the solid lines represent linear fits to the data points

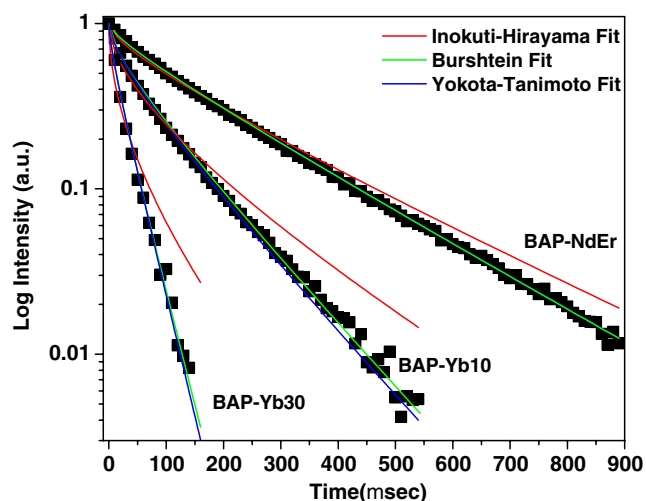


Fig. 8 Experimental decay curves of 887 nm emissions of BAP-NdEr, BAP-Yb10 and BAP-Yb30 glasses with the theoretical fits using inokuti–Hirayama, Burshtein and Yokota–Tanimoto models respectively

BAP-Yb10 and BAP-Yb30 glasses. It is observed that, the fit obtained from Inokuti–Hirayama relation deviates from experimental data both at shorter and longer decay times suggesting that the donor–acceptor energy transfer may not be direct but assisted by donor–donor energy migration. Thus, considering the possibility of energy migration among donor ions, Burshtein’s hopping model Eq. 5 and diffusion model of Yokota–Tanimoto, Eq. 6 as given below have been adopted in the donor decay analysis [37, 38].

$$I(t) = I_0 \exp\left(-\frac{t}{\tau_0} - \gamma\sqrt{t} - Wt\right) \quad (5)$$

$$I(t) = I_0 \exp\left[-\frac{t}{\tau_0} - \frac{4\pi}{3} C_A \Gamma\left(1 - \frac{3}{s}\right) (C_{DA}t)^{3/s} \left(\frac{1 + 10.87X + 15.5X^2}{1 + 8.74X}\right)^{\frac{s-3}{s}}\right] \quad (6)$$

$$X = DC_{DA}^{-1/3} t^{2/3}$$

where, γ is energy transfer parameter, W is migration rate, C_{DA} is energy transfer micro-parameter and D is diffusion coefficient. Both Burshtein and Yokota–Tanimoto models resulted in satisfactory fits with the experimental data indicating that donor to acceptor energy transfer is assisted through the donor–donor migration. The donor to acceptor energy transfer parameters such as energy transfer rate (γ^2), energy transfer micro-parameters (C_{DA}) and critical distance (R_0) have been derived from the fitting parameters using the equations as given below [39]

$$\gamma^2 = \left(\frac{C_A}{C_0}\right)^2 \frac{\pi}{\tau_0} \quad (7)$$

$$C_{DA} = \frac{9\gamma^2}{16C_A^2\pi^3} \quad (8)$$

$$R_0 = (C_{DA}\tau_0)^{1/6} \quad (9)$$

The calculated values for all three models have been tabulated in Table 3. The energy transfer rates (γ^2) obtained using Inokuti–Hirayama model are in accordance with those calculated from measured decay times (Table 2). However, for Burshtein and Yokota–Tanimoto model, the energy transfer rate is less, which is due to a fast excitation energy migration among donor ions before transfer to acceptor [40]. Table 3 also lists out the calculated values of donor–donor energy migration parameters like diffusion coefficient, D that signifies the energy migration process among donors involving excitation energy diffusion (Y–T model) and energy migration rate, W that represents the hopping migration (Burshtein model) along with the values of critical concentration (C_0). If the probability of donor–donor energy migration is more than donor–acceptor energy transfer ($C_{DD} \gg C_{DA}$), the energy transfer can be considered to be hopping assisted migration than that of the diffusion assisted.

The donor–donor energy transfer micro-parameter (C_{DD}) has been calculated from the spectral overlap integral of absorption and emission cross-sections using following equation [41].

$$C_{DD} = \frac{3c}{8\pi^4 n^2} \int \sigma_{abs}^D(\lambda) \sigma_{em}^D(\lambda) d\lambda \quad (10)$$

where, c is velocity of light in vacuum, n is refractive index and $\sigma_{abs}^D(\lambda)$ and $\sigma_{em}^D(\lambda)$ are absorption and emission cross-sections of ${}^4F_{3/2} \leftrightarrow {}^4I_{9/2}$ transitions of Nd^{3+} ion respectively. For Nd^{3+} ions, the self-quenching is supposed to be expected through two paths. First is the cross relaxation (CR) process which involves the de-population of ${}^4F_{3/2}$ level via following transitions: ${}^4F_{3/2} : {}^4I_{9/2} \rightarrow {}^4I_{15/2} : {}^4I_{15/2}$. The second process may be the resonant energy transfer (RET) migration between the nearest neighbor excited and ground state dopant ions through ${}^4F_{3/2} : {}^4I_{9/2} \rightarrow {}^4I_{9/2} : {}^4F_{3/2}$ transitions. The second process is considered here to analyze the donor–donor (Nd^{3+} – Nd^{3+}) energy migration by solving Eq. 10 as described above. The obtained value of energy migration micro-parameter (C_{DD}) is $3.84 \times 10^{-39} \text{ cm}^6 \text{ sec}^{-1}$ and the corresponding critical distance is found to be 10.3 Å. The donor–acceptor energy transfer micro-parameter (C_{DA}) for Nd^{3+} singly and co-doped samples obtained from the theoretical models (Eqs. 4, 5 &

Table 3 The experimental values of Energy transfer parameter (γ), Transfer rate (γ^2), Critical concentration (C_0), Energy transfer micro-parameter (C_{DA}), Critical distance (R_0), Migration rate (W) and Diffusion coefficient (D) obtained from different models for Nd^{3+} emission decay at 887 nm in barium-alumino-metaphosphate glasses on 806 nm excitation

Glass	γ (sec ^{-1/2})	γ^2 (sec ⁻¹)	C_0 (10 ²⁰ ions/cm ³)	C_{DA} (10 ⁻⁴⁰ cm ⁶ sec ⁻¹)	R_0 (Å)	W (sec ⁻¹)	D (10 ⁻¹¹ cm ² sec ⁻¹)
Inokuti–Hirayama (Eq. 4)							
BAP-Nd	4.73	22.38	60.7	0.049	3.4	–	–
BAP-NdEr	38.40	1,474.9	7.38	3.31	6.8	–	–
BAP-Yb05	91.01	8,282.5	4.59	8.57	8.0	–	–
BAP-Yb10	105.57	11,145.82	5.19	6.68	7.7	–	–
BAP-Yb20	175.19	30,690.8	4.65	8.35	8.0	–	–
BAP-Yb30	231.96	53,805.7	4.62	8.43	8.0	–	–
Burshtein (Eq. 5)							
BAP-Nd	4.72	22.56	60.45	0.049	3.4	0.543	–
BAP-NdEr	26.92	724.68	10.53	1.62	6.1	830	–
BAP-Yb05	60.18	3,621.43	6.94	3.74	7.0	2,820	–
BAP-Yb10	67.20	4,515.84	8.16	2.71	6.6	3,790	–
BAP-Yb20	101.99	10,401.96	7.98	2.83	6.7	9,570	–
BAP-Yb30	110.10	12,166.09	9.72	1.91	6.3	21,980	–
Yokota–Tanimoto (Eq. 6)							
BAP-Nd	4.73	22.37	60.71	0.049	3.4	–	–
BAP-NdEr	29.14	849.14	9.73	1.905	6.2	–	0.40
BAP-Yb05	65.72	4,319.12	6.35	4.467	7.2	–	0.91
BAP-Yb10	73.93	5,465.64	7.42	3.277	6.9	–	1.01
BAP-Yb20	113.84	12,958.54	7.15	3.526	6.9	–	1.94
BAP-Yb30	114.47	13,103.38	9.37	2.054	6.4	–	4.45
Spectral Overlap (Eq. 10)							
BAP-Nd			2.12	38.4	10.3		

6) adopted in present study are ranging in the order of 10^{-42} – 10^{-40} cm⁶sec⁻¹, which is less than the donor–donor energy migration micro-parameter ($C_{DD} \sim 10^{-39}$ cm⁶sec⁻¹). This demonstrates that the donor–donor energy migration is dominant over donor–acceptor energy transfer. Thus as stated above, energy transfer in the present Nd^{3+} – Yb^{3+} – Er^{3+} co-doped barium-alumino-metaphosphate glasses can be attributed to the hopping assisted migration among donors followed by donor–acceptor energy transfer. The critical distance (R_0) for Nd^{3+} luminescence quenching has been increased for co-doped samples. The Nd^{3+} – Nd^{3+} critical distance of self-quenching (~ 3.4 Å) is very small compared to that of Nd^{3+} – Er^{3+} (~ 6.1 Å) and Nd^{3+} – Yb^{3+} – Er^{3+} (~ 6.7 Å) signifying the increase in donor–acceptor energy transfer for co-doped samples.

Similarly, to have an understanding on the $Yb^{3+} \rightarrow Er^{3+}$ energy transfer, the Yb^{3+} fluorescence decay curves have also been recorded monitoring emission at 976 nm upon 806 nm excitation and are shown in Fig. 9. From this figure it can be seen that, the time resolved decay spectrum of BAP-NdYb glass shows an initial rise followed by a slow decay with a lifetime of 1.324 ms implying the energy transfer from Nd^{3+} . In the presence of Er^{3+} , the decay

curves show sharp decrease without any initial rise time, which is due to $Yb^{3+} \rightarrow Er^{3+}$ energy transfer. Any further increase in Yb_2O_3 with constant Nd_2O_3 and Er_2O_3 concentration, more decrease in its decay time has been

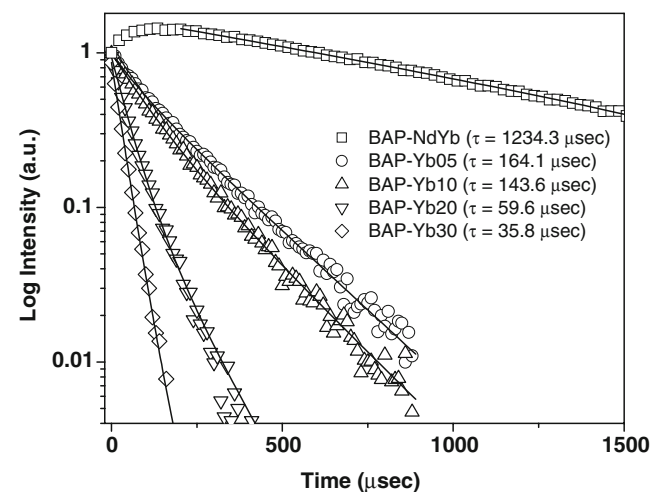


Fig. 9 Decay curves of Yb^{3+} emission at 976 nm with $\lambda_{ex}=806$ nm. Solid lines are the exponential fits to data points used for lifetime calculation

observed and the decay time falls drastically for the glasses with Yb_2O_3 above 1 mol%. This situation is again due to an increased Yb^{3+} – Yb^{3+} energy migration [31]. This energy migration among Yb^{3+} ions increases the efficiency of energy transfer from Yb^{3+} to Er^{3+} ions.

Conclusion

It could be concluded that a new series of barium-alumino-metaphosphate glasses single/dual/triply doped with Nd^{3+} – Yb^{3+} – Er^{3+} ions have successfully been prepared and analyzed their emission, excitation and fluorescence decay characteristics. The Yb^{3+} ions are found to be providing efficient bridging action for Nd^{3+} to Er^{3+} energy transfer. A fourfold emission enhancement at 1,542 nm of Er^{3+} has been achieved in the presence of Yb^{3+} ions while excitation through $^4\text{I}_{9/2} \rightarrow ^4\text{F}_{5/2}$ transition of Nd^{3+} at 806 nm from barium-alumino-metaphosphate glass with 3 mol% Yb_2O_3 resulting in an energy transfer efficiency of 94%. Emission enhancement of Er^{3+} has satisfactorily been explained based on energy transfer from Nd^{3+} to Er^{3+} through Yb^{3+} ions by the application of Inokuti–Hirayama (direct energy transfer), Burshtein (hopping assisted migration) and Yokota–Tanimoto (diffusion assisted migration) theoretical models on the experimental decay kinetics. It has been observed from the time resolved fluorescence decay of donor ion that the energy transfer between donor and acceptor ions could be attributed to the hopping assisted migration among donors followed by donor–acceptor energy transfer through electrostatic dipole–dipole interactions.

Acknowledgements Authors would like to thank Dr. H. S. Maiti, Director, CGCRI for his kind encouragement and permission to publish this work which is carried out under an In-house project No. MLP0101. Our thanks are also due to Dr. Ranjan Sen, for his kind support in the present work. One of us (Mr.A.D.S.) is thankful to the CGCRI, CSIR for the award of Research Internship to him.

References

- Hwang BC, Jiang S, Luo T, Watson J, Sorbello G, Peyghambarian N (2000) *J Opt Soc Am B* 17:833–839
- Golding PS, Jackson SD, King TA, Polnau M (2000) *Phys Rev B* 62:856–864
- Sinha G, Patra A (2009) *Chem Phys Lett* 473:151–154
- Lin H, Liu XR, Pun EYB (2002) *Opt Mater* 18:397–401
- Solarz P, Ryba-Romanowski W (2007) *Radiat Meas* 42:759–762
- Noginov MA, Curley M, Noginova N, Wang WS, Aggarwal MD (1998) *Appl Opt* 37:5737–5742
- Jiang C, Jin L (2009) *Appl Opt* 48:2220–2227
- Tin P, Schearer LD (1990) *J Appl Phys* 68:950–953
- Jonas EH, Björn J, Valdas P, Fredrik L (2007) *Optics Express* 15:13930–13935
- Watekar PR, Seongmin Ju, Han W-T (2006) *IEEE Photon Tech Lett* 18:1609–1611
- Davidov BL, Krylov AA (2007) *Quantum Electron* 37:843–846
- Liegard F, Doualan JL, Moncorge R, Bettinelli M (2005) *Appl Phys B* 80:985–991
- Zhao YW, Lin YF, Chen YJ, Gong XH, Luo ZD, Huang YD (2008) *Appl Phys B* 90:461–464
- Hwang B-C, Jiang S, Luo T, Watson J, Sorbello G, Peyghambarian N (2000) *J Opt Soc Am B* 17:833–839
- Lin H, Jiang S, Wu J, Song F, Peyghambarian N, Pun EYB (2003) *J Phys D Appl Phys* 36:812–817
- Shi WQ, Bass M (1989) *J Opt Soc Am B* 6:23–29
- Campbel JH, Suratwala TI (2000) *J Non-cryst Solids* 263–264:318–341
- Moustafa YM, El-Egili K (1998) *J non-cryst Solids* 240:144–153
- Machado IEC, Prado L, Gomes L, Prison JM, Martinelli JR (2004) *J Non-Cryst Solids* 348:113–117
- Fleming JW Jr, Shiever JW (1981) United States Patent 4302074
- Lee ETY, Taylor ERM (2004) *J Phys Chem Solids* 65:1187–1192
- Capobianco JA, Proulx PP, Bettinelli M, Negrisolo F (1990) *Phys Rev B* 42:5936–5944
- Ahmad MM, Hogarth EA, Khan MN (1984) *J Mater Sci* 19:4041–4044
- A. J. Glass laser program annual report (1975) Lawrence-Livermore Labs. Report No. URCL-50021-72
- Jundt DH (1997) *Opt Lett* 22:1553–1555
- Choi JH, Shi FG, Margaryan A, Margaryan A (2005) *J Mater Res* 20:264–270
- Carnall WT, Fields PR, Rajnak K (1968) *J Chem Phys* 49:4424–4442
- Salley GM, Valiente R, Gudel HU (2002) *J Phys Condens Matter* 14:5461–5475
- Gruber JB, Sardar DK, Zandi B, Hutchinson JA, Trussell CW (2003) *J Appl Phys* 93:3137–3140
- Rotman SR (1990) *Opt Lett* 15:230–232
- Shi WQ, Kurtz R, Machan J, Bass M, Birnbaum M, Kokta M (1987) *Appl Phys Lett* 51:1218–1220
- Fujii T, Kodaira K, Kawauchi O, Tanaka N, Yamashita H, Anpo M (1997) *J Phys Chem B* 101:10631–10637
- Hebbink GA, Grave L, Woldering LA, Reinhoudt DN, van Veggel FCMJ (2003) *J Phys Chem A* 107:2483–2491
- Diaz-Tores LA, Barbosa-Garcia O, Struck CW, McFarlane RA (1998) *J Lumin* 78:69–86
- Park JK, Kim CH, Han CH, Park HD, Choi SY (2003) *Electrochem Solid-State Lett* 6:H13–H15
- Inokuti M, Hirayama F (1965) *J Chem Phys* 43:1978–1989
- Burshtein AI (1972) *Sov Phys JETP* 35:882–891
- Martin IR, Rodriguez VD, Rodriguez-Mendoza UR, Lavin V, Montoya E, Jaque D (1999) *J Chem Phys* 111:1191–1194
- da Vila LD, Gomes L, Tarelho LVG, Ribeiro SJL, Messedeq Y (2003) *J Appl Phys* 93:3873–3880
- da Vila LD, Gomes L, Tarelho LVJ, Ribeiro SJL, Messaddeq Y (2004) *J Appl Phys* 95:5451–5463
- Braud A, Girald S, Doualan JL, Moncorge R (1998) *IEEE J Quantum Electron* 34:2246–2255